Original Article

RGMB-AS1/miR-4428/PBX1 axis drives the progression of cervical cancer

Chenge Shen[1], Beixi Wang[2], Kaiwen Zhang[3], Ce Wang[4], Jiajia Wang[5], Zhanglu An[1], Lisha Shu[6]

[1]Department of Obstetrics and Gynecology, Hebei North University, Zhangjiakou 075000, China; [2]Department of Pathology, Xinxiang Medical University, Xinxiang 453003, China; [3]Department of Obstetrics and Gynecology, Zhengzhou University, Zhengzhou 450000, China; [4]Department of Human Anatomy and Histology and Embryology, [5]Department of Pathology, Hebei North University, Zhangjiakou 075000, China; [6]Department of Obstetrics and Gynecology, the First Affiliated Hospital of Hebei North University, Zhangjiakou 075000, China

Contributions: (I) Conception and design: C Shen; (II) Administrative support: L Shu; (III) Provision of study materials or patients: L Shu; (IV) Collection and assembly of data: B Wang; (V) Data analysis and interpretation: K Zhang; (VI) Manuscript writing: All authors; (VII) Final approval of manuscript: All authors.

Correspondence to: Lisha Shu. Department of Obstetrics and Gynecology, the First Affiliated Hospital of Hebei North University, Qiaoxi District, Zhangjiakou 075000, China. Email: shumil1448114@163.com.

Background: RGMB antisense RNA 1 (*RGMB-AS1*) is a member of long non-coding RNAs (lncRNAs) and relates to the carcinogenesis of numerous cancers. Nonetheless, its performance and mechanism in cervical cancer (CC) is unclear.

Methods: The expressions of *RGMB-AS1*, microRNA-4428 (*miR-4428*), PBX homeobox 1 (*PBX1*) were analyzed by quantitative real-time PCR (qRT-PCR). Nuclear-cytoplasmic fractionation was used to locate *RGMB-AS1*. Cell counting kit-8 (CCK-8), EdU, TUNEL, Western blot and transwell assays were performed to assess *RGMB-AS1* function in proliferation, apoptosis, and invasion *in vitro*. Interplays involving *miR-4428*, *RGMB-AS1* and *PBX1* were verified applying luciferase reporter, RNA pull-down and RNA immunoprecipitation (RIP).

Results: *RGMB-AS1* level was high in CC specimens and cells. *RGMB-AS1* encouraged proliferation, and invasion, and depressed apoptosis in CC cells. Further, *miR-4428* was screened as a targeted for *RGMB-AS1*, and *RGMB-AS1* performed the competitive endogenous RNA (ceRNA) role to release *PBX1* from *miR-4428*. Correlation analysis based on clinical specimens confirmed positive association between *RGMB-AS1* and *PBX1* and negative association of *miR-4428* with *RGMB-AS1* and *PBX1*. Rescue experiments indicated that *PBX1* overexpression counteracted *RGMB-AS1* silence-caused inhibition on CC development.

Conclusions: *RGMB-AS1* regulated *miR-4428/PBX1* axis to aggravate CC development, indicating that targeting *RGMB-AS1* could be a potent way for developing the novel therapeutic methods for CC patients.

Keywords: RGMB antisense RNA 1 (*RGMB-AS1*); microRNA-4428 (*miR-4428*); PBX homeobox 1 (*PBX1*); cervical cancer (CC)

Submitted Nov 28, 2019. Accepted for publication Mar 30, 2020.
doi: 10.21037/tcr.2020.04.19
View this article at: http://dx.doi.org/10.21037/tcr.2020.04.19

Introduction

CC has the fourth highest morbidity and mortality in cancers (1). This year has seen an increase of about 570,000 diagnoses and 310,000 deaths of CC cases in the world (2). Although CC treatment has been developed for the patients, the prognosis of CC patients is still unoptimistic (3). Hence, mechanism in CC is imperative to be understood so that the therapeutic method for CC could be improved.

Long non-coding RNA (lncRNA) is a newly proposed non-coding RNA (ncRNA) whose length is over 200 nucleotides, and is engaged in regulating cancer progression

(4,5). For example, lncRNA HOXD-AS1 enhances the proliferative and invasive capacity of melanoma cells through inhibiting RUNX3 expression (6). Moreover, lncRNA SUMO1P3 facilitates tumor growth, distant metastasis and angiogenesis in colon cancer (7). ZEB1-AS1 shows oncogenic behaviors in gastric cancer and predicts an unfavorable prognosis (8). Numerous recent reports have demonstrated that lncRNA containing miRNA response element (MRE) elicit competitive endogenous RNA (ceRNA) function through sequestering target miRNAs at the MREs (9-11). Interestingly, various lncRNAs functioning as ceRNA are largely documented in CC. For instance, LINC00473 promotes CC tumorigenesis by targeting miR-34a and preventing ILF2 degradation (12). SNHG16, a sponge of miR-216-5p, contributes to the migration and invasion of CC cells through regulating ZEB1 (13). In addition, CASC2/miR-21/PTEN axis modulates cisplatin sensitivity of CC (14). It was discovered that RGMB antisense RNA 1 (*RGMB-AS1*) showed oncogenic property in cancers such glioma (15), laryngeal squamous carcinoma (16), and lung adenocarcinoma (17). However, no report has linked *RBMB-AS1* to CC yet.

The aim of this research was to inquire the biological role and possible mechanism of *RGMB-AS1* in CC. We identified marked upregulation of *RGMB-AS1* in CC tissues and cells and demonstrated that *RGBM-AS1* elicited promoting function of in proliferation, apoptosis and invasion of CC cells via regulating microRNA-4428 (*miR-4428*)/PBX homeobox 1 (*PBX1*) axis.

Methods

Human tissue samples

All patients (n=32) were diagnosed with CC in the First Affiliated Hospital of Hebei North University Prior to this study, and these patients did not receive any other treatment. Fresh CC tissues and corresponding para-tumor tissues were gained from abovementioned participants hospitalized from May 2013 to December 2018. Fresh tissues were frozen in liquid nitrogen immediately after resection and stored at –80 ℃. Written informed consent was signed by every patient and this experiment gained permission from ethics committee of the First Affiliated Hospital of Hebei North University (approval number: 1809036).

Cell culture

Human cervical epithelial cell (H8) and CC cells (HeLa, C-33A, SiHa and CaSki) were bought from Chinese Academy of Sciences (Beijing, China). A RPMI-1640 medium (Invitrogen, Carlsbad, USA) containing 10% FBS (Invitrogen) plus 1% penicillin/streptomycin (Sigma-Aldrich, Milan, Italy) was applied to culture above cells. A moist environment of 5% CO_2 at 37 ℃ was required for culturing. Besides, medium was replaced every 3 days.

Cell transfection

Specific shRNAs against *RGMB-AS1* (sh-*RGMB-AS1*#1 and sh-*RGMB-AS1*#2) with corresponding negative control (sh-NC), and the pcDNA3.1 vector targeting *RGMB-AS1* or *PBX1* and with negative control vector, were gained from Genechem (Shanghai, China). Moreover, *miR-4428* mimics and NC mimics were gained from GenePharma (Shanghai, China). Above plasmids were separately transfected into SiHa or CaSki cells utilizing Lipofectamine 3000 (Invitrogen, Carlsbad, USA).

Quantitative real-time PCR (qRT-PCR)

Isolation of cellular RNA was finished via TRIZOL (Invitrogen, Carlsbad, USA) and cDNA was synthesized by iScript^{TM} Reverse Transcription Supermix (Bio-Rad, Hercules, CA, USA). Samples were sequentially analyzed with SYBR Green Master Mix (Vazyme, Nanjing, China) on ABI 7500 Realtime PCR system (Applied Biosystems, Foster City, CA, USA). Fold changes of target genes were calculated as per $2^{-\Delta\Delta Ct}$ method and GAPDH or U6 served as the endogenous calibrator control.

Cell counting kit-8 (CCK-8) assay

Cell proliferation was explored with CCK-8 (Dojindo, Kumamoto, Japan). Transfected SiHa or CaSki cells were inoculated into 96-well plates, and cultured overnight. Upon this, before detection, each well was supplemented with 10 µL CCK-8 solutions. Values at 450 nm were examined through the Epoch Microplate Spectrophotometer (Bio Tek, Winooski, VT, USA) upon culture for 0, 24, 48, 72 and 96 h, respectively.

Western blot

Total protein was obtained from transfected SiHa or CaSki cells which were lysed by radio immunoprecipitation assay (RIPA) lysis buffer (Beyotime, Jiangsu, China). Subsequently, protein was quantified by using the BCA assay kit (Beyotime). The dodecyl sulfate, sodium salt (SDS)-polyacrylamide gel electrophoresis (PAGE) was performed on proteins from lysates which were then moved to polyvinylidene fluoride membranes (PVDF; Millipore, Bedford, MA, USA). Membranes were cultured with primary antibodies overnight at 4 ℃, and antibodies used were as follows: anti-Bcl-2 (ab32124, Abcam, Cambridge, USA), anti-Bax (ab32503, Abcam), anti-MMP2 (ab215986, Abcam), anti-MMP9 (ab219372, Abcam), anti-*PBX1* (ab97994, Abcam) and anti-GAPDH (ab97994, Abcam). Then, secondary antibodies were added for cultivation for 1 h in dark room. Finally, the proteins were detected by an Enhanced Chemiluminescence Detection Kit (Millipore, Bedford, MA, USA).

Terminal dexynucleotidyl transferase (TdT)-mediated dUTP nick end labeling assay

The apoptosis of transfected SiHa or CaSki cells was assessed via a TUNEL Apoptosis Kit (Invitrogen, Carlsbad, USA). Cells were dyed with DAPI (Koritai, Beijing, China). Then, cells were observed and images were captured by using a fluorescence microscopy (Olympus, Tokyo, Japan).

5-ethynyl-2'-deoxyuridine (EdU) assay

Transfected CaSki or SiHa cells were seeded into fresh 96-well plates for cultivation. After incubation with EdU (Sigma-Aldrich, St. Louis, MO, USA) for 2 h, the cells were fixed by using 4% PFA (Solarbio, Beijing, China) and dyed in Apollo Dye Solution (RiboBio, Guangdong, China). Nucleic acid was stained with Hoechst 33342 stain (Invitrogen, Carlsbad, USA). Images were captured under an inverted fluorescence microscope (Carl Zeiss, Jena, Germany) and the proportion of EdU-positive cells was determined.

Cell invasion assay

Cell invasion was studied utilizing the 24-well Transwell system (Corning Costar, Cambridge, MA, USA). Transfected SiHa or CaSki cells were trypsinized and suspended in serum-free medium and subsequently added to the upper chamber of the Transwell system with Matrigel (BD Biosciences, San Jose, CA, USA). A 0.6 mL medium with additional 10% FBS was plated to the lower chamber. Cells were cultured for 24 h for invasion test. Invasive cells were fixed and stained utilizing crystal violet (Richard-Allan Scientific, San Diego, CA, USA), followed by washed twice using PBS (Sigma-Aldrich). Stained cells were eventually observed by an inverted microscope (Olympus Co., Tokyo, Japan).

Subcellular fractionation

For separating nuclear and cytoplasmic fraction, RNAs from SiHa or CaSki cells were isolated with the PARIS kit (Thermo Fisher Scientific, Waltham, MA, USA). The RNA expression level of *RGMB-AS1* in nuclear and cytoplasmic fractions was explored using qRT-PCR.

Luciferase reporter assay

RGMB-AS1-WT/Mut or *PBX1*-WT/Mut was sub-cloned into the pmirGLO dual-luciferase vector (Promega, Madison, WI, USA) so as to generate pmirGLO-*RGMB-AS1*-WT/Mut or pmirGLO-*PBX1*-WT/Mut. The pmirGLO-*RGMB-AS1*-WT/Mut was co-transfected into SiHa or CaSki cells with *miR-4428* mimics or NC mimics. The pmirGLO-*PBX1*-WT/Mut was co-transfected into SiHa or CaSki cells with *miR-4428* mimics or *miR-4428* mimics + pcDNA3.1/*RGMB-AS1* or NC mimics. At 48 h post-transfection, dual luciferase reporter assay system (Promega, Madison, WI, USA) was applied to examine luciferase activities.

RNA pull-down

SiHa or CaSki cells were lysed using lysis buffer and incubated with Bio-*miR-4428*-WT/Mut or Bio-NC, followed by incubation with streptavidin-coupled magnetic beads (Invitrogen). *RGMB-AS1* and *PBX1* levels were individually studied by qRT-PCR.

RNA immunoprecipitation (RIP)

RIP analysis was conducted in SiHa or CaSki cells using the Magna RIP RNA-Binding Protein Immunoprecipitation Kit (Millipore, Bedford, MA, USA). Cells were lysed in RIP buffer. The resulting cell extraction was incubated with ProteinA/G magnetic beads bounded to anti-Ago2 (Abcam, Cambridge, UK) or anti-IgG (Abcam). Enrichment levels of *RGMB-AS1*, *miR-4428* and *PBX1* were individually measured with qRT-PCR.

Statistical analysis

Data were expressed as means ± SD. Statistical analysis was conducted using the SPSS (IBM, Armonk, NY, USA). Significance of the variance between two or several groups was evaluated by Student's *t*-test or one-way ANOVA. Correlation among *RGMB-AS1*, *miR-4428* and *PBX1* was assessed by Pearson's correlation analysis. P<0.05 was regarded as statistically significant in general. The experiments were conducted for at least thrice.

Results

RGMB-AS1 is overexpressed in HCC and facilitates CC cell proliferation, invasion and restrained cell apoptosis

To explore the expression pattern of *RGMB-AS1* in CC tissues and cell lines (HeLa, C-33A, SiHa, CaSki), qRT-PCR analysis was conducted. The adjacent non-tumor tissues and cervical epithelial cell (H8) were utilized as negative controls, separately. As a result, *RGMB-AS1* expression was dramatically elevated in CC tissues (*Figure 1A*). Consistently, the high *RGMB-AS1* level was found in CC cell lines (*Figure 1B*). To estimate the role of *RGMB-AS1* in CC cells, *RGMB-AS1* was knocked down by sh-*RGMB-AS1*#1 and sh-*RGMB-AS1*#2 (*Figure 1C*). Then, CCK-8 data and EdU-labeling results indicated that SiHa and CaSki cell proliferation was remarkably reduced by *RGMB-AS1* knockdown of (*Figure 1D,E*). Later, the impact of *RGMB-AS1* depletion on cell apoptosis was evaluated. Shown by the result of TUNEL assay, *RGMB-AS1* deficiency significantly encouraged apoptosis of SiHa and CaSki cells (*Figure 1F*). The reduced Bcl-2 and increased Bax protein levels upon *RGMB-AS1* silence were observed with Western blot assay, further verifying that cell apoptosis was promoted by *RGMB-AS1* knockdown (*Figure 1G*). Moreover, transwell assay depicted decreased invasion ability in SiHa and CaSki cells (*Figure 1H*). Lastly, the effect of *RGMB-AS1* on the proteins that related to metastasis were assessed. The results showed that silenced *RGMB-AS1* considerably restrained the levels of MMP2 and MMP9 proteins (*Figure 1I*). Additionally, *RGBM-AS1* was overexpressed by pcDNA3.1/*RGMB-AS1* in HeLa and C-33A cells which expressed relatively low *RGMB-AS1* level (*Figure S1A*). Then, we discovered that overexpressing *RGMB-AS1* drive proliferation and depressed apoptosis in 2 cell lines (*Figure S1B,C,D*). Accordingly, Bcl-2 level upregulated and Bax level de-regulated under *RGMB-AS2* overexpression (*Figure S1E*). Invasion of HeLa and C-33A cells was weakened upon *RGMB-AS1* overexpression (*Figure S1F*), and MMP2 and MMP9 levels declined with *RGMB-AS1* overexpression as well (*Figure S1G*). Conclusively, *RGMB-AS1* is overexpressed in HCC and facilitates CC cell proliferation, invasion and restrained cell apoptosis.

RGMB-AS1 was associated with miR-4428 by acting as a sponge

Mounting reports have suggested that lncRNAs and miRNAs were closely linked to regulate biological processes (18,19). To confirm whether *RGMB-AS1* played regulatory role in CC via functioning as a ceRNA, its cellular localization was detected. As a result, *RGMB-AS1* was more in cytoplasm than in nucleus (*Figure 2A*). Hence, we hypothesized that *RGMB-AS1* might serve as a ceRNA in cytoplasm Thereafter, we applied StarBase tool (http://starbase.sysu.edu.cn/agoClipRNA.php?source=lncRNA&flag=target&clade=mammal&genome=human&assembly=hg19&miRNA=all&clipNum=1&deNum=0&panNum=0&target=RGMB-AS1) to search potential miRNAs for *RGMB-AS1*. The results manifested five miRNAs (miR-574-3p, miR-3614-5p, miR-670-3p, *miR-4428* and miR-22-3p) that could interact with *RGMB-AS1* (*Figure 2B*). As illustrated in *Figure 2C*, only *miR-4428* expression was notably increased in CC cells transfected with sh-*RGMB-AS1*#1. Therefore, *miR-4428* was selected for the following investigation. To confirm the relationship between *miR-4428* and CC, *miR-4428* expression was measured with qRT-PCR analysis. The result displayed that *miR-4428* expression was obviously under-expressed in CC tissues and cells versus the corresponding normal tissues and cervical epithelium (*Figure 2D,E*). Then, we verified the elevated *miR-4428* expression after transfecting *miR-4428* mimics in 2 CC cell lines (*Figure 2F*). Based on StarBase prediction, a *miR-4428* binding site in *RGMB-AS1* was recognized, and we mutated this site for further detection (*Figure 2G*). Consequently, the luciferase activity for *RGMB-AS1*-WT declined evidently under *miR-4428* overexpression, but that of *RGMB-AS1*-Mut was unchanged (*Figure 2H*). RNA pull-down assay uncovered that *RGMB-AS1* was pulled down by *miR-4428*-WT rather than *miR-4428*-Mut biotinylated probe (*Figure 2I*). At last, the negative relevance between *RGMB-AS1* and *miR-4428*

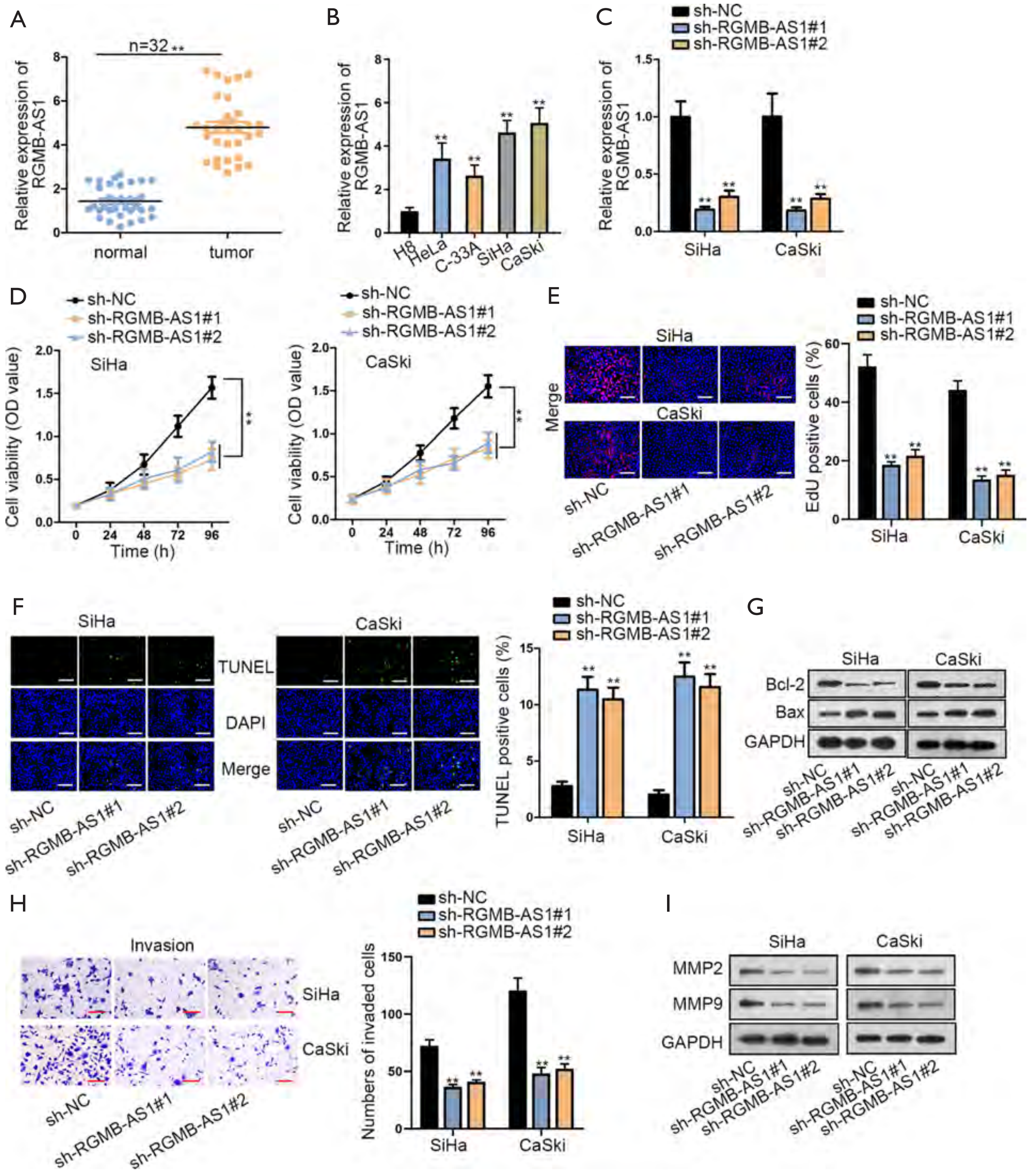

Figure 1 Expression and function of *RGMB-AS1* in CC. (A) *RGMB-AS1* expression in CC tissues and corresponding normal tissues was detected by qRT-PCR; (B) qRT-PCR data of *RGMB-AS1* expression in four CC cell lines, HeLa, C-33A, SiHa, CaSki, and cervical epithelium, H8 (control); (C) *RGMB-AS1* expression was tested by qRT-PCR in CC cells with sh-*RGMB-AS1*#1/2/3 transfection; (D,E) CCK-8 test of viable SiHa and CaSki cells and EdU staining of proliferative SiHa and CaSki cells with *RGMB-AS1* knockdown. Scale bar: 50 μm; (F) TUNEL-labeled CC cells was imaged and calculated under *RGMB-AS1* silence. Scale bar: 100 μm; (G) Western blot of Bax and Bcl-2 in CC cells with *RGMB-AS1* knockdown; (H) the invaded SiHa and CaSki cells in a transwell system was imaged and counted under *RGMB-AS1* knockdown. Scale bar: 100 μm; (I) Western blots of MMP2 and MMP9 proteins in CC cells with *RGMB-AS1* deficiency. **, P<0.01. RGMB-AS1, RGMB antisense RNA 1; CC, cervical cancer; qRT-PCR, quantitative real-time PCR; CCK-8, cell counting kit-8.

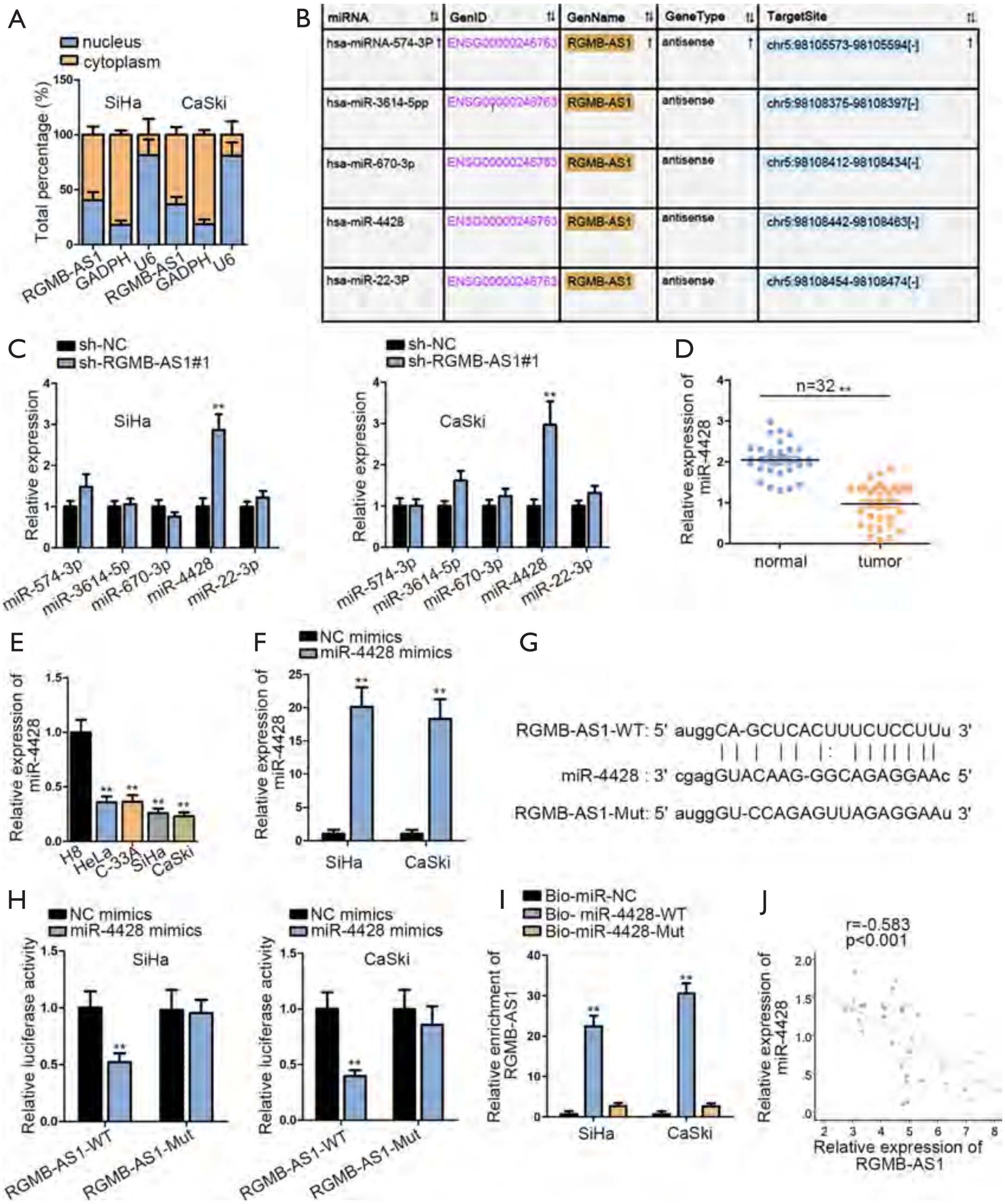

miRNA	GenID	GenName	GeneType	TargetSite
hsa-miRNA-574-3P	ENSG00000246763	RGMB-AS1	antisense	chr5:98105573-98105594[-]
hsa-miR-3614-5pp	ENSG00000246763	RGMB-AS1	antisense	chr5:98108375-98108397[-]
hsa-miR-670-3p	ENSG00000246763	RGMB-AS1	antisense	chr5:98108412-98108434[-]
hsa-miR-4428	ENSG00000246763	RGMB-AS1	antisense	chr5:98108442-98108463[-]
hsa-miR-22-3P	ENSG00000246763	RGMB-AS1	antisense	chr5:98108454-98108474[-]

Figure 2 *RGMB-AS1* sponged *miR-4428*. (A) The distribution of *RGMB-AS1* in SiHa and CaSki cells was conformed through subcellular localization; (B) StarBase predicted the potential miRNAs (miR-574-3p, miR-3614-5p, miR-670-3p, *miR-4428* and miR-22-3p) interacting with *RGMB-AS1*; (C) qRT-PCR data of the levels of potential miRNAs (miR-574-3p, miR-3614-5p, miR-670-3p, *miR-4428* and miR-22-3p) in CC cells with *RGMB-AS1* silence; (D) qRT-PCR was utilized to detect *miR-4428* expression in CC tissues and adjacent normal tissues; (E) the expression of *miR-4428* in CC cell lines (HeLa, C-33A, SiHa, CaSki) was determined by qRT-PCR. The control is cervical epithelium (H8); (F) the transfection efficiency of *miR-4428* mimics was examined using qRT-PCR; (G) prediction of *miR-4428* sites in *RGMB-AS1* was obtained from StarBase; (H) luciferase activity pmirGLO-*RGMB-AS1*-WT or pmirGLO-*RGMB-AS1*-Mut reporter was measured in two CC cells introduced with and NC or *miR-4428* mimics; (I) SiHa and CasKi cells lysates were mixed with Bio-*miR-4428*-WT or Bio-*miR-4428*-Mut for RNA pull-down and *RGMB-AS1* level in the pulldown products were detected; (J) the correlation between the expression of *RGMB-AS1* and *miR-4428* was analyzed with the employment of Pearson's correlation analysis. **, P<0.01. RGMB-AS1, RGMB antisense RNA 1; miR-4428, microRNA-4428; qRT-PCR, quantitative real-time PCR; CC, cervical cancer.

was recognized in CC tissues (*Figure 2J*). Taken together, *RGMB-AS1* interacted with *miR-4428* as a sponge.

RGMB-AS1 upregulated PBX1 by sponging miR-4428

To support the hypothesis of ceRNA mechanism, we subsequently searched the downstream mRNAs for *miR-4428* using StarBase with the setting of 3 prediction programs (RNA22, miRmap and microT). The Venn diagram showed that there are 16 potential mRNAs for *miR-4428* (*Figure 3A*). qRT-PCR analysis showed that among 16 candidate genes, *PBX1* exhibited the most significant upregulation in 3 CC specimens versus corresponding para-tumor normal ones (*Figure S2*). *PBX1* was commonly reported as oncogene (20-22), so we speculated *PBX1* as the target for *miR-4428* in CC. qRT-PCR analysis confirmed the upregulated *PBX1* in 32 CC tissues and 4 cell lines (*Figure 3B*,*C*). Then, effects of *RGMB-AS1* and *miR-4428* on PBM1 were measured. As presented in *Figure 3D*,*E*, the levels of *PBX1* mRNA and protein were diminished with the transfection of sh-*RGMB-AS1*#1/2. Besides, *miR-4428* mimics observably attenuated *PBX1* mRNA and protein levels (*Figure 3F*,*G*). Then, the overexpression of *RGMB-AS1* by pcDNA3.1/*RGMB-AS1* in CC cells was confirmed by qRT-PCR (*Figure 3H*). Moreover, as shown in *Figure 3I*, RIP assay demonstrated that *RGMB-AS1*, *miR-4428* and *PBX1* could be detected in Ago2 immunoprecipitates rather than IgG (*Figure 3I*). In addition, luciferase reporter assay confirmed that the decrease of *PBX1*-WT luciferase activity caused by *miR-4428* mimics was restored by *RGMB-AS1* overexpression, but no evident difference was discovered in *PBX1*-Mut (*Figure 3J*). RNA pull-down assay further validated that both *RGMB-AS1* and *PBX1* were pulled down by *miR-4428*-WT, rather than *miR-4428*-Mut (*Figure 3K*). Furthermore, *PBX1* expression was positively associate with *RGMB-AS1* and negatively related to *miR-4428* in CC specimens (*Figure 3L*). Jointly, *RGMB-AS1* regulates *PBX1* by sponging *miR-4428*.

RGMB-AS1 enhances CC progression through regulating PBX1

Finally, we tested whether *PBX1* was a target for *RGMB-AS1* to regulate CC cellular activities. We first used pcDNA3.1/*PBX1* to increase the expression of *PBX1* so as to unfold rescue experiments (*Figure 4A*). Later, we showed that the proliferative ability of CC cells was restrained by the silence of *RGMB-AS1* and was recovered by *PBX1* overexpression (*Figure 4B*,*C*). Besides, TUNEL staining suggested that the promoting effect of *RGMB-AS1* silence on CC cell apoptosis was offset by transfecting pcDNA3.1/*PBX1* through TUNEL (*Figure 4D*). Decreased Bcl-2 and increased Bax in CC cells with *RGMB-AS1* silence were reversed by *PBX1* overexpression (*Figure 4E*). According to transwell assay, overexpressing *PBX1* countervailed the repressive impact of *RGMB-AS1* depletion on CC cell migration (*Figure 4F*). Additionally, silenced *RGMB-AS1* lessened the levels of MMP2 and MMP9, while the transfection of pcDNA3.1/*PBX1* reversed the effect of silenced *RGMB-AS1* (*Figure 4G*). In brief, *RGMB-AS1* enhances CC progression through regulating *PBX1*.

Discussion

It was proposed that lncRNAs could function as regulators in the biological processes, including cancers. Recent studies have revealed that lncRNAs might act as sponges for miRNAs in cancer progression (23). Several lncRNA-miRNA axes are revealed in cancers, such as MALAT1-miR-218 axis in choriocarcinoma (24), NEAT1-miR-181a-5p in lung cancer (25), and PVT1-miR-128-3p axis in CC (26). Data form previous volumes supported that *RGMB-AS1* is activated by E2F1 and enhances papillary thyroid carcinoma cell proliferation and invasion (27). *RGMB-AS1* is also associated with clinical stage in hepatocellular carcinoma (28). *RGMB-AS1* indicates an unfavorable prognosis in lung adenocarcinoma and regulates its progression (17). Hence, we assumed that *RGMB-AS1* might participate in CC. Expectedly, our study first suggested that *RGMB-AS1* was significant overexpressed in CC tissues and cells. *RGMB-AS1* knockdown lessened proliferation and invasion, and increased apoptosis, whereas its overexpression had opposite effects. These data consistently implied the oncogenic property of *RGMB-AS1* in CC.

MiRNAs are a kind of short RNAs with 21–25 nucleotides (29). MiRNA serves as tumor promoters or tumor suppressors in tumorigenesis and development of cancers (30,31). For instance, miRNA-518 represses cell growth and induces apoptosis in gastric cancer via targeting MDM2. MiR-183 is overexpressed in glioblastoma and downregulates LRIG1 expression to promote glioblastoma radioresistance (32). MiRNA-423 promotes hepatocellular carcinoma cell invasion via regulating BRMS1 (33). A variety of miRNAs was reported to relate to CC progression. For example, miRNA-433 represses CC tumor size and distant metastasis

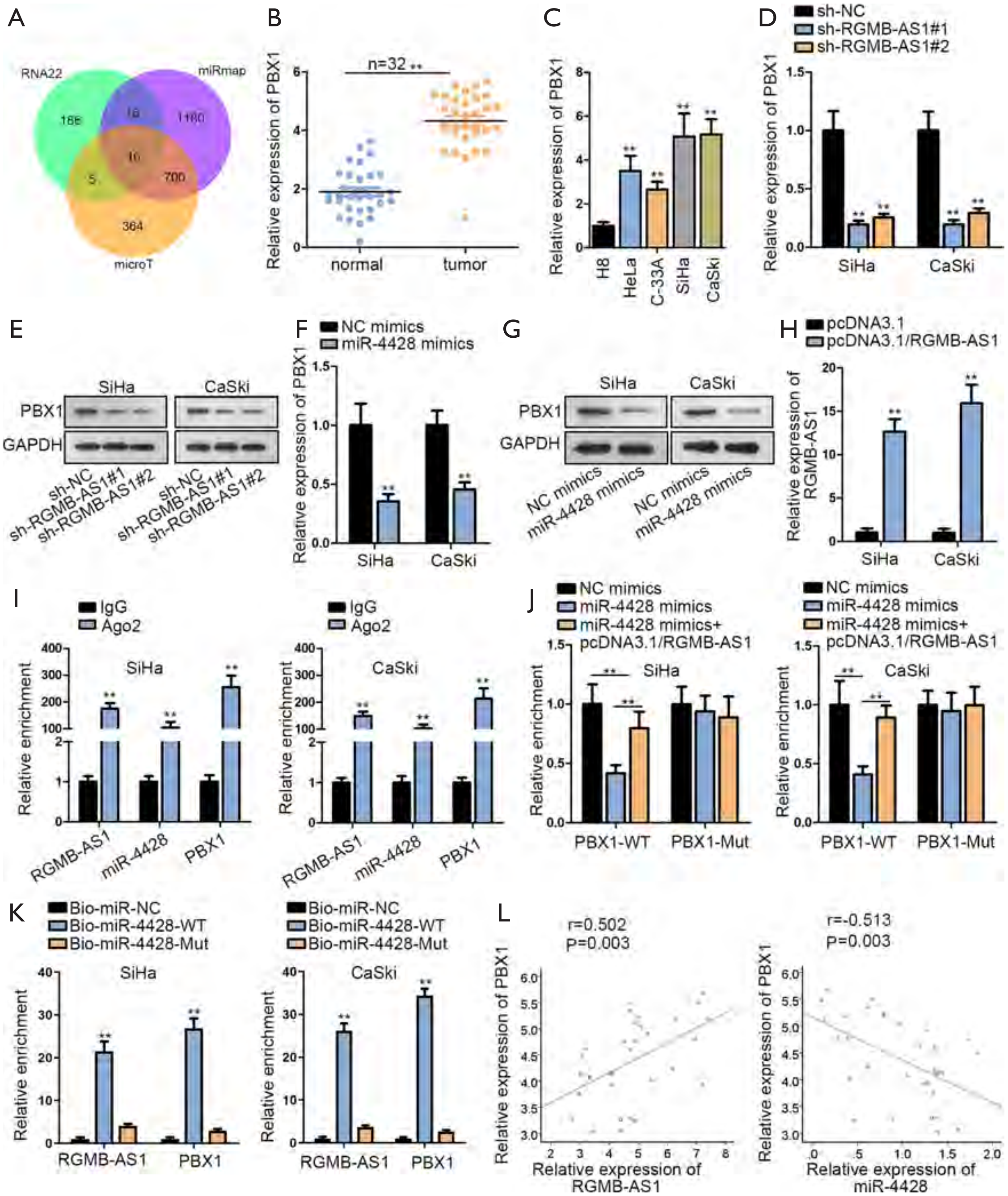

Figure 3 *MiR-4428* targets to *PBX1*. (A) The Venn diagram showed the potential mRNAs binding with *miR-4428* from StarBase; (B) *PBX1* expression in CC tissues and matched normal tissues was detected by qRT-PCR; (C) qRT-PCR and Western blot data of *PBX1* expression in four CC cell lines and one normal cell line; (D,E) *PBX1* mRNA and protein levels were examined by qRT-PCR and Western blot in CC cells transfected with sh-*RGMB-AS1*#1/2; (F,G) qRT-PCR and Western blot data of *PBX1* mRNA and protein under *miR-4428* mimics transfection in CC cells; (H) qRT-PCR of *RGMB-AS1* level in CC cells transfected with pcDNA3.1/*RGMB-AS1* versus pcDNA3.1; (I) enrichments of *RGMB-AS1*, *miR-4428* and *PBX1* bound in Ago2 RIP was estimated by qRT-PCR. IgG was negative reference; (J) luciferase activity of *PBX1*-WT and *PBX1*-Mut was measured in CC cells transfected *miR-4428* mimics and *miR-4428* mimics + pcDNA3.1/*RGMB-AS1*; (K) *RGMB-AS1* and *PBX1* enrichment was evaluated by qRT-PCR in the pulldown of bio-*miR-4428*-WT/Mut; (L) expression correlation of *PBX1* with *RGMB-AS1* and *miR-4428* was tested by Pearson's correlation analysis in CC tissues. **, P<0.01. miR-4428, microRNA-4428; PBX1, PBX homeobox 1; CC, cervical cancer; qRT-PCR, quantitative real-time PCR; RGMB-AS1, RGMB antisense RNA 1; RIP, RNA immunoprecipitation.

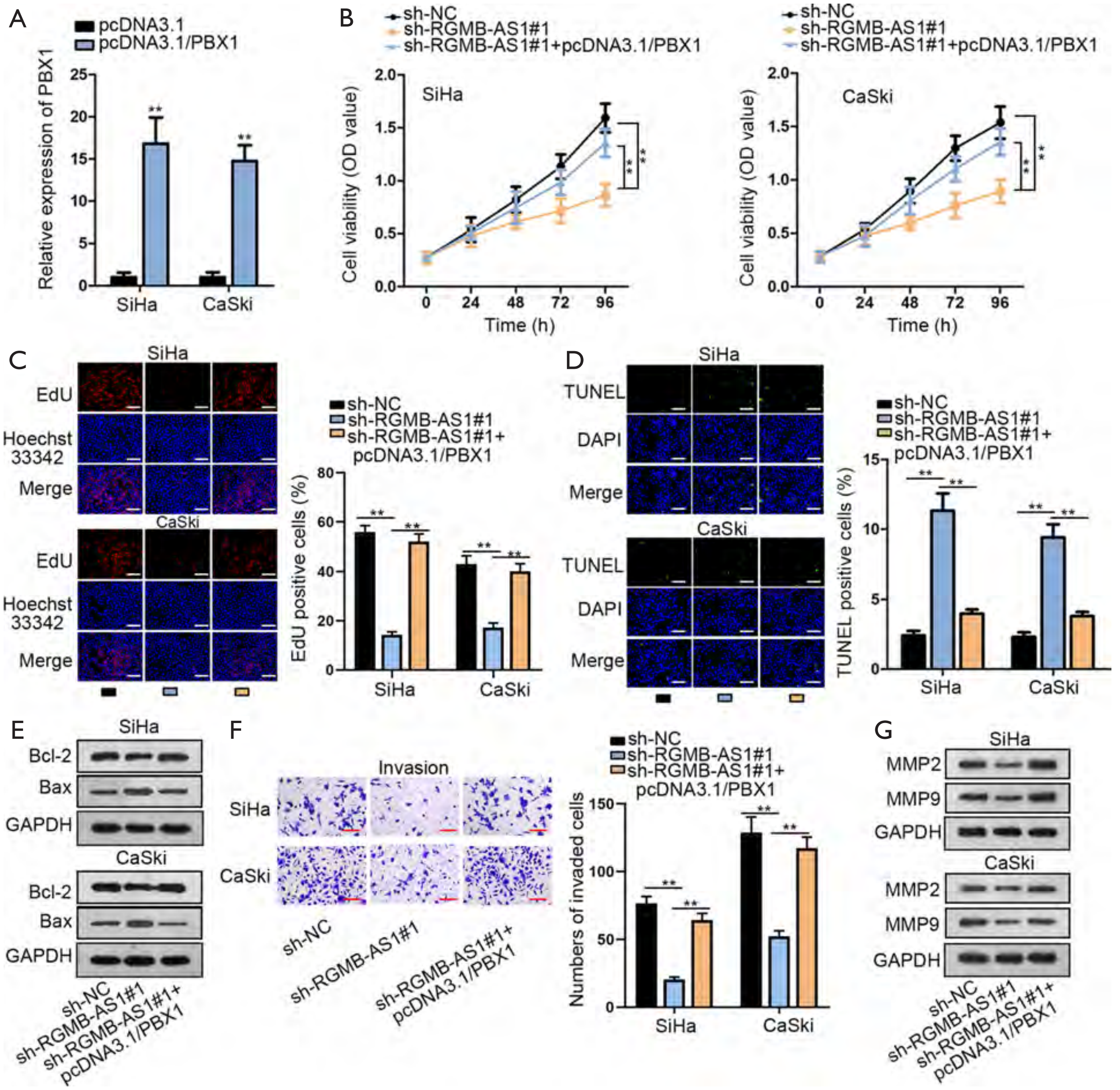

Figure 4 *RGMB-AS1* enhanced CC progression through regulating *PBX1*. (A) The transfection efficiency of pcDNA3.1/*PBX1* was tested by qRT-PCR; (B,C) cell proliferation was tested by CCK-8 and EdU in CC cells transfected with sh-NC, sh-*RGMB-AS1*#1 or sh-*RGMB-AS1*#1 + pcDNA3.1/*PBX1*. Scale bar: 50 μm; (D) images of TUNEL-labeled apoptotic CC cells in each group. Scale bar: 100 μm; (E) Western blot of Bax and Bcl-2 in CC cells of each group; (F) cell invasion in cells transfected with sh-NC, sh-*RGMB-AS1*#1 or sh-*RGMB-AS1*#1 + pcDNA3.1/*PBX1* was determined by transwell assay. Scale bar: 100 μm; (G) MMP2 and MMP9 protein levels in CC cells of each group was estimated by Western blot assay. **, P<0.01. RGMB-AS1, RGMB antisense RNA 1; CC, cervical cancer; PBX1, PBX homeobox 1; qRT-PCR, quantitative real-time PCR; CCK-8, cell counting kit-8.

by regulating the AKT/β-catenin signaling pathway and targeting to metadherin (34). MicroRNA-150 targets to PDCD4 in CC and boosts cell proliferation, migration and invasion (35). MiR-214 enhances the drug sensitivity of CC via regulating FOXM1 (36). *MiR-4428* is first identified as a downregulated miRNA in CC tissues and cells. Further, we first predicted and demonstrated that *RGMB-AS1* directly combine with *miR-4428* via putative MRE. Moreover, we first exhibited that *RGMB-AS1* expression was negatively correlated with *miR-4428* expression in CC. Thus, we provided first data to link *RGMB-AS1* to *miR-4428* in CC.

Further, we found that *PBX1* was a target for *miR-4428* and upregulated overtly in CC. As formerly reported, *PBX1* promotes the proliferation of clear cell renal carcinoma by JAK2/STAT3 signaling (20). *PBX1* is upregulated in breast cancer and plays essential role in the regulation of breast cancer development (21). *PBX1* serves as a stem cell reprogramming factor and modulates the chemoresistance of ovarian cancer (22). However, the role and mechanism of *PBX1* in CC is first explained by our study. We showed that both *RGMB-AS1* knockdown and *miR-4428* overexpression could decline the expression of *PBX1*. Importantly, we found that *RGMB-AS1* regulates *PBX1* expression by sponging *miR-4428*. Moreover, we delineated the positive relevance between *RGMB-AS1* and *PBX1* and the negative relevance between *miR-4428* and *PBX1*. According to rescue experiments, *PBX1* overexpression restored *RGMB-AS1* depletion-mediated repressing effect on CC progression, indicating that *PBX1* was a target for *RGMB-AS1* to regulate CC.

Conclusively, *RGMB-AS1* contributes to CC progression through acting as a ceRNA, and *RGMB-AS1/miR-4428/PBX1* axis could offer an inspiring thought for the therapy in CC patients.

Acknowledgments

We appreciate all the participants who provide supports in this study.
Funding: None.

Footnote

Conflicts of Interest: All authors have completed the ICMJE uniform disclosure form (available at http://dx.doi.org/10.21037/tcr.2020.04.19). The authors have no conflicts of interest to declare.

Ethical Statement: The authors are accountable for all aspects of the work in ensuring that questions related to the accuracy or integrity of any part of the work are appropriately investigated and resolved. Written informed consent was signed by every patient and this experiment gained permission from ethics committee of the First Affiliated Hospital of Hebei North University (approval number: 1809036).

References

1. Musselwhite LW, Oliveira CM, Kwaramba T, et al. Racial/ethnic disparities in cervical cancer screening and outcomes. Acta Cytol 2016;60:518-26.
2. Bray F, Ferlay J, Soerjomataram I, et al. Global cancer statistics 2018: GLOBOCAN estimates of incidence and mortality worldwide for 36 cancers in 185 countries. CA Cancer J Clin 2018;68:394-424.
3. Wentzensen N, Schiffman M. Accelerating cervical cancer control and prevention. Lancet Public Health 2018;3:e6-7.
4. Wang Z, Yang B, Zhang M, et al. lncRNA epigenetic landscape analysis identifies EPIC1 as an oncogenic lncRNA that interacts with MYC and promotes cell-cycle progression in cancer. Cancer Cell 2018;33:706-20.e9.
5. Li J, Liu C. Coding or noncoding, the converging concepts of RNAs. Front Genet 2019;10:496.
6. Zhang H, Bai M, Zeng A, et al. LncRNA HOXD-AS1 promotes melanoma cell proliferation and invasion by suppressing RUNX3 expression. Am J Cancer Res 2017;7:2526-35.
7. Zhang LM, Wang P, Liu XM, et al. LncRNA SUMO1P3 drives colon cancer growth, metastasis and angiogenesis. Am J Transl Res 2017;9:5461-72.
8. Li Y, Wen X, Wang L, et al. LncRNA ZEB1-AS1 predicts unfavorable prognosis in gastric cancer. Surg Oncol 2017;26:527-34.
9. Furió-Tarí P, Tarazona S, Gabaldón T, et al. spongeScan: A web for detecting microRNA binding elements in lncRNA sequences. Nucleic Acids Res 2016;44:W176-80.
10. Qu J, Li M, Zhong W, et al. Competing endogenous RNA in cancer: a new pattern of gene expression regulation. Int J Clin Exp Med 2015;8:17110-6.
11. He X, Guo S, Wang Y, et al. Systematic identification and analysis of heat-stress-responsive lncRNAs, circRNAs and miRNAs with associated co-expression and ceRNA networks in cucumber (Cucumis sativus L.). Physiol Plant 2020;168:736-54.

12. Shi C, Yang Y, Yu J, et al. The long noncoding RNA LINC00473, a target of microRNA 34a, promotes tumorigenesis by inhibiting ILF2 degradation in cervical cancer. Am J Cancer Res 2017;7:2157-68.
13. Zhu H, Zeng Y, Zhou CC, et al. SNHG16/miR-216-5p/ZEB1 signal pathway contributes to the tumorigenesis of cervical cancer cells. Arch Biochem Biophys 2018;637:1-8.
14. Feng Y, Zou W, Hu C, et al. Modulation of CASC2/miR-21/PTEN pathway sensitizes cervical cancer to cisplatin. Arch Biochem Biophys 2017;623-624:20-30.
15. Pan B, Zhao M, Wang N, et al. LncRNA RGMB-AS1 promotes glioma growth and invasion through miR-1200/HOXB2 axis. Onco Targets Ther 2019;12:10107-14.
16. Xu Z, Xi K. LncRNA RGMB-AS1 promotes laryngeal squamous cell carcinoma cells progression via sponging miR-22/NLRP3 axis. Biomed Pharmacother 2019;118:109222.
17. Li P, Zhang G, Li J, et al. Long noncoding RNA RGMB-AS1 indicates a poor prognosis and modulates cell proliferation, migration and invasion in lung adenocarcinoma. PLoS One 2016;11:e0150790.
18. Sanchez Calle A, Kawamura Y, Yamamoto Y, et al. Emerging roles of long non-coding RNA in cancer. Cancer Sci 2018;109:2093-100.
19. Wei W, Liu Y, Lu Y, et al. LncRNA XIST promotes pancreatic cancer proliferation through miR-133a/EGFR. J Cell Biochem 2017;118:3349-58.
20. Wei X, Yu L, Li Y. PBX1 promotes the cell proliferation via JAK2/STAT3 signaling in clear cell renal carcinoma. Biochem Biophys Res Commun 2018;500:650-7.
21. Wang J, Shidfar A, Ivancic D, et al. Overexpression of lipid metabolism genes and PBX1 in the contralateral breasts of women with estrogen receptor-negative breast cancer. Int J Cancer 2017;140:2484-97.
22. Jung JG, Shih IM, Park JT, et al. Ovarian cancer chemoresistance relies on the stem cell reprogramming factor PBX1. Cancer Res 2016;76:6351-61.
23. Xu W, Yu S, Xiong J, et al. CeRNA regulatory network-based analysis to study the roles of noncoding RNAs in the pathogenesis of intrahepatic cholangiocellular carcinoma. Aging (Albany NY) 2020;12:1047-86.
24. Shi D, Zhang Y, Lu R, et al. The long non-coding RNA MALAT1 interacted with miR-218 modulates choriocarcinoma growth by targeting Fbxw8. Biomed Pharmacother 2018;97:543-50.
25. Li S, Yang J, Xia Y, et al. Long noncoding RNA NEAT1 promotes proliferation and invasion via targeting miR-181a-5p in non-small cell lung cancer. Oncol Res 2018;26:289-96.
26. Gao YL, Zhao ZS, Zhang MY, et al. Long noncoding RNA PVT1 facilitates cervical cancer progression via negative regulating of miR-424. Oncol Res 2017;25:1391-8.
27. Zhang Z, Li SY, Zhang LB. LncRNA RGMB-AS1 is activated by E2F1 and promotes cell proliferation and invasion in papillary thyroid carcinoma. Eur Rev Med Pharmacol Sci 2018;22:1979-86.
28. Sheng N, Li Y, Qian R, et al. The clinical significance and biological function of lncRNA RGMB-AS1 in hepatocellular carcinoma. Biomed Pharmacother 2018;98:577-84.
29. Mohr S, Doebele C, Comoglio F, et al. Hoxa9 and Meis1 cooperatively induce addiction to Syk signaling by suppressing miR-146a in acute myeloid leukemia. Cancer Cell 2017;31:549-62.e11.
30. Lan H, Lu H, Wang X, et al. MicroRNAs as potential biomarkers in cancer: opportunities and challenges. Biomed Res Int 2015;2015:125094.
31. Wang Y, Wang B, Zhou H, et al. MicroRNA-384 inhibits the progression of papillary thyroid cancer by targeting PRKACB. Biomed Res Int 2020;2020:4983420.
32. Fan H, Yuan R, Cheng S, et al. Overexpressed miR-183 promoted glioblastoma radioresistance via down-regulating LRIG1. Biomed Pharmacother 2018;97:1554-63.
33. Sun X, Wang M, Liu H, et al. MicroRNA-423 enhances the invasiveness of hepatocellular carcinoma via regulation of BRMS1. Am J Transl Res 2017;9:5576-84.
34. Liang C, Ding J, Yang Y, et al. MicroRNA-433 inhibits cervical cancer progression by directly targeting metadherin to regulate the AKT and β-catenin signalling pathways. Oncol Rep 2017;38:3639-49.
35. Zhang Z, Wang J, Li J, et al. MicroRNA-150 promotes cell proliferation, migration, and invasion of cervical cancer through targeting PDCD4. Biomed Pharmacother 2018;97:511-7.
36. Wang JM, Ju BH, Pan CJ, et al. MiR-214 inhibits cell migration, invasion and promotes the drug sensitivity in human cervical cancer by targeting FOXM1. Am J Transl Res 2017;9:3541-57.

Cite this article as: Shen C, Wang B, Zhang K, Wang C, Wang J, An Z, Shu L. *RGMB-AS1/miR-4428/PBX1* axis drives the progression of cervical cancer. Transl Cancer Res 2020;9(5):3180-3190. doi: 10.21037/tcr.2020.04.19

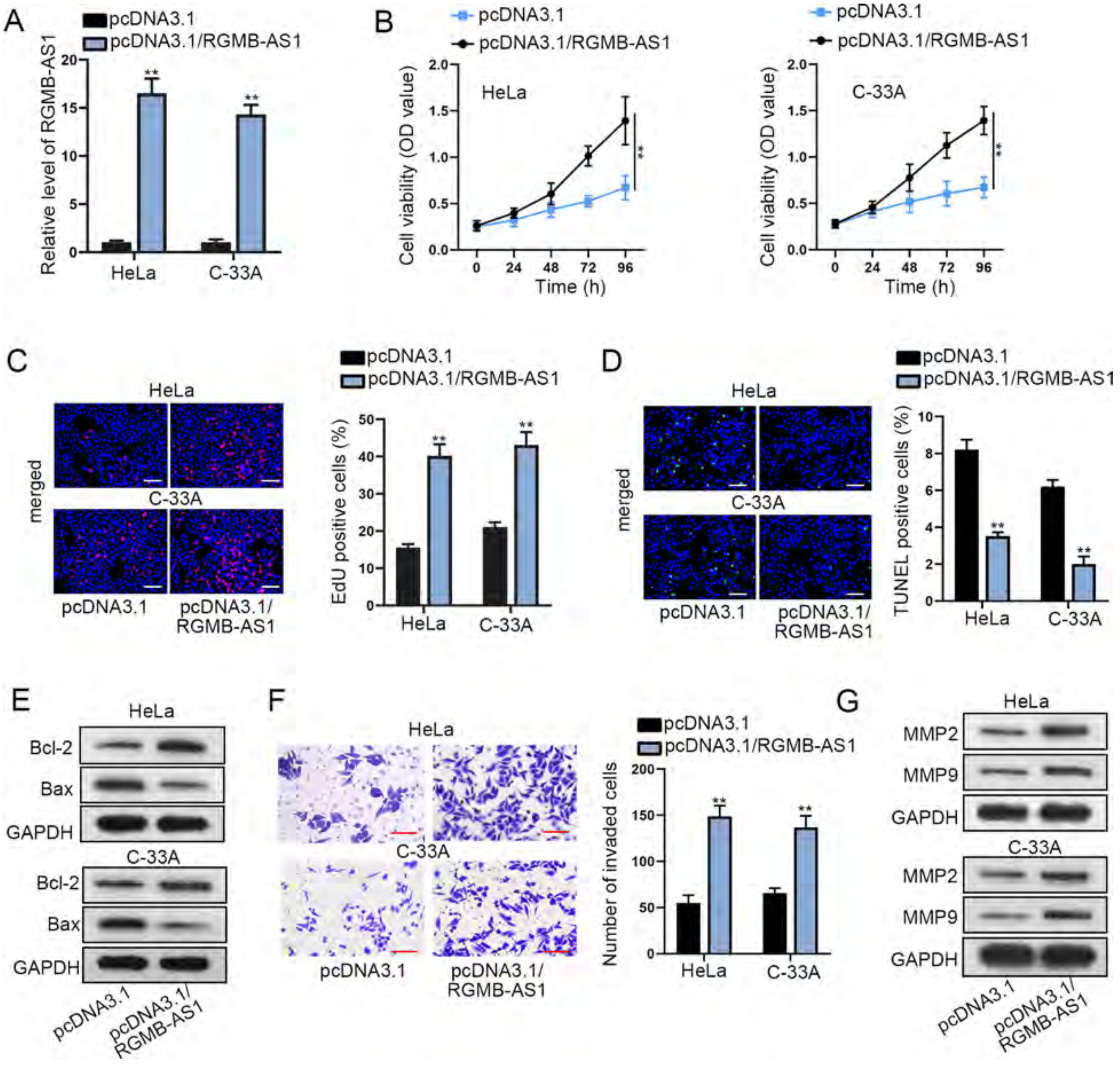

Figure S1 Effect of *RGMB-AS1* overexpression on CC cells. (A) *RGMB-AS1* expression in CC cells transfected with pcDNA3.1/*RGMB-AS1* was evaluated by qRT-PCR; (B,C) proliferation of CC cells with *RGMB-AS1* overexpression was estimated by CCK-8 and EdU. Scale bar: 50 μm; (D) TUNEL-labeled apoptotic CC cells with *RGMB-AS1* overexpression was imaged and evaluated. Scale bar: 100 μm; (E) Western blot tested Bcl-2 and Bax level in CC cells under *RGMB-AS1* overexpression; (F) invasion of CC cells under *RGMB-AS1* overexpression was tested by transwell assay. Scale bar: 100 μm; (G) Western blot of MMP2 and MMP9 in CC cells under *RGMB-AS1* overexpression. **, P<0.01. RGMB-AS1, RGMB antisense RNA 1; CC, cervical cancer; qRT-PCR, quantitative real-time PCR; CCK-8, cell counting kit-8.

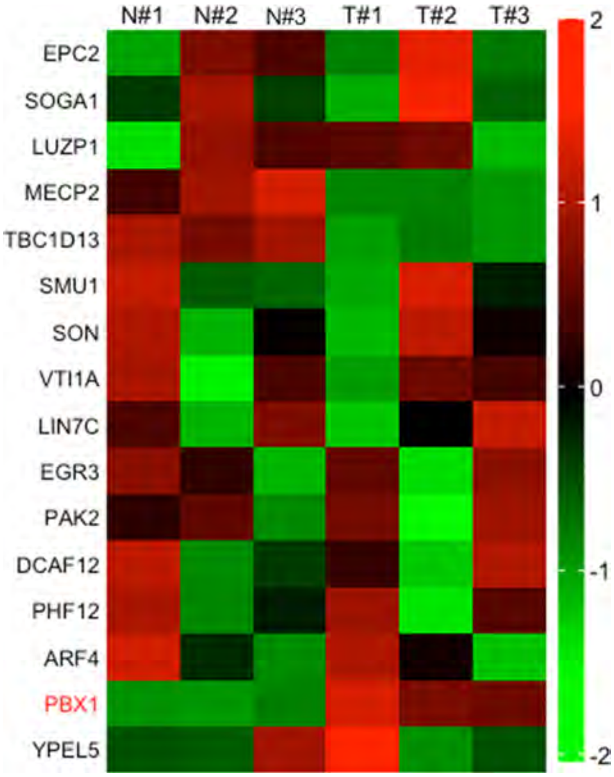

Figure S2 Expressions of candidate genes in CC specimens. Heat-map showed the qRT-PCR levels of 16 candidate miR-4428 target genes in 3 CC tissues versus para-tumor ones. CC, cervical cancer; qRT-PCR, quantitative real-time PCR; miR-4428, microRNA-4428.